Modeling and Sensitivity Analysis of Compressor Stations in Gas Transport Simulations

Anton Baldin
Fraunhofer Institute for Algorithms and Scientific Computing
Sankt Augustin, Germany
email: Anton.Baldin@scai.fraunhofer.de

Kläre Cassirer
Fraunhofer Institute for Algorithms and Scientific Computing
Sankt Augustin, Germany
email: Klaere.Cassirer@scai.fraunhofer.de

Tanja Clees
University of Applied Sciences Bonn-Rhein-Sieg and Fraunhofer Institute for Algorithms and Scientific Computing
Sankt Augustin, Germany
email: Tanja.Clees@scai.fraunhofer.de

Bernhard Klaassen
Fraunhofer Institute for Algorithms and Scientific Computing
Sankt Augustin, Germany
email: Bernhard.Klaassen@scai.fraunhofer.de

Igor Nikitin
Fraunhofer Institute for Algorithms and Scientific Computing
Sankt Augustin, Germany
email: Igor.Nikitin@scai.fraunhofer.de

Lialia Nikitina
Fraunhofer Institute for Algorithms and Scientific Computing
Sankt Augustin, Germany
email: Lialia.Nikitina@scai.fraunhofer.de

Sabine Pott
Fraunhofer Institute for Algorithms and Scientific Computing
Sankt Augustin, Germany
email: Sabine.Pott@scai.fraunhofer.de

***Abstract*—This paper describes the mathematical modeling of compressors used in gas transport networks. Compressors of various types (piston, generic, turbo), different levels of modeling (free, advanced), as well as their combinations into compressor stations (serial, parallel) are considered. Particular attention is paid to the questions of global convergence and stability of the result to the variations of starting point and other parameters of the solution procedure. Sensitivity Analysis and Principal Component Analysis for stationary gas transport problems are considered. A number of numerical experiments on realistic scenarios confirm the conclusions of the theoretical analysis.**

***Index Terms*—simulation and modeling; mathematical and numerical algorithms and methods; advanced applications; gas transport networks; sensitivity analysis; principal component analysis**

I. Introduction

This work is an extension of our conference paper [1], where gas compressors of piston and generic type have been considered. For the sake of completeness, we have added a review of the main results of the paper [2] on turbine compressors. Also, we present a detailed review of [3] results on Sensitivity Analysis (SA) and Principal Component Analysis (PCA) of gas transport simulations and supplement it with new numerical experiments.

In this paper, we will continue the study of globally converging methods for solving stationary network problems on the example of gas transport networks. In our earlier work [4], we introduced the concept of generalized resistivity of network elements and formulated stability conditions for the algorithm solving the corresponding network problems. Under these conditions, for arbitrary variation of the starting point, the solution procedure converges to the same or numerically close result. The approach is universal and can be applied also, e.g., for water transport and electric power networks [5]. In the works [2], [6], [7] we have considered in detail the modeling of gas compressors of the turbine type. For these compressors, individually calibrated characteristics and data resampling on a regular grid were used. In the present paper, we consider compressors of piston and generic type, which are characterized by the existence of analytical solutions and a simpler representation of control equations. This simulation extends our system MYNTS (Multi-phYsics NeTwork Simulator).

Globally convergent method of solution of stationary network problems in applications to electric networks was formulated in [8]. The method has been designed for piecewise linear systems of equations. The space of variables was subdivided to polyhedral cells, where the system has been represented by a non-degenerate linear mapping, with continuous connection on the boundary. The method converges from an arbitrary starting point to a unique solution, in a finite number of steps. Further, in [9], the method has been extended to the linear mappings that can be degenerate in finite cells. In [10], these systems have been represented in min-max or equivalent abs-normal form and several methods for their solution have been discussed. In application to smooth nonlinear systems, the piecewise linear mappings can be used as an approximation. However, the methods above increase the number of steps when the cells become smaller and will

perform slowly in practice. The general methods for solution of non-linear systems are described in [11]. In particular, there is a mathematically strict but little-known result, that Newton method equipped with Armijo line search stabilizer provides the global convergence for solution of smooth non-degenerate systems. No methods are known well working for general smooth non-linear systems in the presence of degeneracy.

Modeling of gas transport networks is described in detail in [12], [13]. The real gas networks consist mainly of pipes, and their modeling is based on the nonlinear friction law, simplest by Nikuradse [14], more advanced by Colebrook-White [15] and Hofer [16]. The other parts of the modeling are empirical approximations for the equation of state of a real gas, the simplest by Papay [17], more complex AGA8-DC92 [18] and GERG2008 [19] standards. However, neither pipe nor state equations generally present an obstacle for solving gas transport problems. Rare exceptions are cycles of short pipes where unstable circulations can be excited and regions of phase transitions where jumps and folds of state equation can appear. Otherwise, the pipe and state equations are very smooth and typically solved with several iterations of stabilized Newton method. The problem is presented by compressors and regulators, the elements increasing and decreasing pressure in the network to the desired values. The corresponding element equations make the system piecewise degenerate [4], requiring a development of special methods for its solution. Possible ways for construction of such methods will be discussed in this paper.

In Section II, we recall the general concepts of element resistivity and describe their physical meaning in more detail. In Section III, we will look at compressors of piston, generic and turbine type. In Section IV, we describe Sensitivity Analysis and Principal Component Analysis of gas transport simulations. Section V presents the methods for solving nearly degenerate nonlinear systems. In Section VI, we will carry out a numerical solution of several realistic network problems, presenting the application of the above described methods.

II. Transport variables in stationary network problems

Network problems of a stationary type are described by a system of equations that includes linear Kirchhoff equations of the form $\sum Q_i = 0$, which describe the conservation of flows in network nodes, and equations of elements of the form $f(P_{in}, P_{out}, Q) = 0$, in the general case, nonlinear, introduced on each edge of the network graph. Here the transport variables $P_{in/out}$ are used – nodal variables for the input and output of the element, for gas networks – pressure values, Q – the flow through the element. In gas problems, flows are considered in different normalizations, which is indicated by the index: Q_m – mass flow, Q_ν – molar flow, Q_N – volumetric flow under normal conditions, $Q_{vol,in/out}$ – volumetric flow in input or output conditions (by default, input conditions are taken), etc. An element is called generalized resistive if its equation has derivatives of the following signature:

$$\partial f/\partial P_{in} > 0,\ \partial f/\partial P_{out} < 0,\ \partial f/\partial Q < 0. \qquad (1)$$

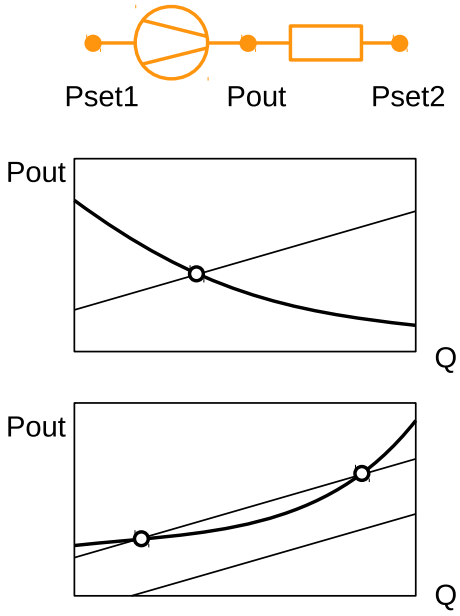

Fig. 1. On the top: a serial connection of compressor (circle) and resistor (rectangle); in the center: decreasing compressor $P_{out}(Q)$ characteristics (thick line) and increasing resistor $P_{out}(Q)$ characteristics (thin line) have a single intersection (stable case); at the bottom: increasing compressor $P_{out}(Q)$ characteristics (thick line) and increasing resistor $P_{out}(Q)$ characteristics (thin lines) can have multiple intersections or no intersection (unstable case). Image from [1].

The work [4] shows that stationary network problems in which all elements have a given signature have a unique solution that can be found by the standard stabilized Newton algorithm with an arbitrary choice of starting point. Technically, it also requires a supply with a set pressure P_{set} in each disconnected component of the graph, as well as a proper condition for the behavior of functions at infinity, which can be satisfied if there are linear continuations of the equations of elements outside the working region that have the signature (1). Also, the completely opposite signature is formally admissible, since the sign change of $f \to -f$ is admissible for stationary problems. To eliminate this trivial ambiguity, one can choose the sign of f, postulating the fulfillment of one of the conditions (1), for example, the first one.

The physical meaning of these conditions is illustrated in Figure 1. It shows the serial connection of the tested element (in this case the compressor, a circle) and a linear resistor (a rectangle). Pressure $P_{set1,2}$ is set at the free ends. The intermediate node must satisfy the equation

$$P_{out}(P_{set1}, Q) = P_{set2} + RQ, \qquad (2)$$

graphically depicted in the central and lower parts of the figure. Here $R > 0$ is the resistance value, the corresponding line on the figure increases monotonically. If the tested element has the signature (1), then the function $P_{out}(P_{set1}, Q)$ decreases monotonically in Q, which corresponds to the central part of the figure. In this case, the intersection of lines exists and is unique. It can also occur outside this graph, when the above condition is met at infinity (continuation of the element's

characteristic by a linearly strictly decreasing function outside the working region). In the case, if the signature (1) would be violated and the function $P_{out}(P_{set1}, Q)$ would increase in Q, then by choosing the parameters P_{set2} and R it is possible to achieve that the lines will have several intersections or no intersection. Even if the function $P_{out}(P_{set1}, Q)$ increases in Q only locally, a linear resistor can be fitted to it, which will give several solutions to the problem under consideration. It is also clear that a nonlinear resistor can also be used for this purpose, as long as its characteristic increases and has enough parameters for tuning.

Similarly, by connecting elements in reverse order, as well as considering their parallel connection, it can be shown that any violation of the condition (1) leads to a violation of the uniqueness of solution. If the signature is violated, then the tested element can be connected to an elementary resistive element in such a way that the equation will have several solutions or none. The case when the signature is satisfied for all elements and the system has a unique solution is, of course, more preferable in practical applications.

Compressors are the most complex elements in gas problems; several levels of modeling are used to represent them. The main purpose of introduction of these levels is the gradual sophistication of modeling, where the solution of a simple model is used as a starting point for the more complex one. Also, it allows to separate effects dependent on individual calibration of compressors from their basic representation.

Free model: is the simplest, formulated only in terms of transport variables, and is described by a piecewise linear formula of the form

$$\begin{aligned} &\max(\min(\ P_{in} - P_L, -P_{out} + P_H, -Q + Q_H), \\ &P_{in} - P_{out}, -Q) + \epsilon(P_{in} - P_{out} - Q) = 0, \end{aligned} \tag{3}$$

where parameters P_L, P_H, Q_H define target values, for example, $P_H = SPO$ for specified output pressure, or upper and lower limits for other controlled values. This formula defines a polyhedral surface in the space of transport variables in the so-called *maxmin* representation [10]. Typical surface is shown below on Figure 2 left. The last term, controlled by small positive parameter ϵ, serves regularization and will be explained below.

Advanced model: introduces additional internal variables for compressors: revolution number rev, adiabatic enthalpy increase H_{ad}, performance $Perf$, efficiency η, torque M_t, and additional equations:

$$P = \rho RTz/\mu,\ Q_m = Q_{vol}\rho_{in}, \tag{4}$$

$$H_{ad} = P_{in}/(\rho_{in}\alpha) \cdot ((P_{out}/P_{in})^{\alpha} - 1), \tag{5}$$

$$Perf = Q_m H_{ad}/\eta,\ M_t = Perf/(2\pi \cdot rev), \tag{6}$$

$$\alpha = (\kappa - 1)/\kappa,\ 0 < \alpha < 1,\ 0 < \eta < 1, \tag{7}$$

where the equation of state is written first with its parameters: density ρ, universal gas constant R, absolute temperature T, compressibility factor z, molar mass μ; the second is the relationship between the mass flow and the volumetric flow in the input conditions; the following are definitions of internal variables in terms of transport variables; $\kappa > 1$ is the adiabatic exponent.

The advanced model also introduces additional patches, inserted into the free formula (3) as follows:

$$\begin{aligned} &\max(\min(\ P_{in} - P_L, -P_{out} + P_H, -Q + Q_H, \\ &\qquad \underline{f_1, ..., f_n}\ ), \\ &P_{in} - P_{out}, -Q) + \epsilon(P_{in} - P_{out} - Q) = 0. \end{aligned} \tag{8}$$

The additional patches for various types of compressors are described below. The general strategy is to resolve all internal variables from the corresponding equations, obtain a formula in terms of transport variables, check its signature, and use it in the standard solution algorithm.

III. Gas compressors

Three different types of compressors are considered.

A. Piston compressors

Compressors of piston types are modeled by direct proportionality

$$Q_{vol} = V \cdot rev \tag{9}$$

with given constants η and V – compressor chamber volume. The control equation has the following patches:

$$f_1 = rev_{max} - rev \geq 0, \tag{10}$$

$$f_2 = M_{t,max} - M_t \geq 0, \tag{11}$$

$$f_3 = Perf_{max} - Perf \geq 0, \tag{12}$$

$$f_4 = rel_{max} - P_{out}/P_{in} \geq 0, \tag{13}$$

$$f_5 = \Delta P_{max} - (P_{out} - P_{in}) \geq 0, \tag{14}$$

with given constants rev_{max}, $M_{t,max}$, rel_{max}, ΔP_{max} and the function $Perf_{max}(rev)$ determined by the characteristics of the compressor drive.

Stability analysis: calculating the derivatives of f_i with respect to (P_{in}, P_{out}, Q_m) in the working region $0 < P_{in} \leq P_{out}$, $Q_m > 0$, $rev > 0$, we get the signatures given in Table I. In this case, the above formulas are used, as well as the stability of the equation of state: $\rho > 0$, $\partial\rho/\partial P > 0$. In particular, $rev = Q_m/(\rho_{in}V)$ has signature $(-0+)$, which implies the signature of f_1 in the table. $M_t = H_{ad}\rho_{in}V/(2\pi\eta)$ has signature $(* + 0)$, where $* = \partial(H_{ad}\rho_{in})/\partial P_{in} < 0$ for $P_{out}/P_{in} < (1 - \alpha)^{(-1/\alpha)} = \beta$. Thus, the signature f_2 is correct only if the compressor raises the pressure by no more than the factor β, with the value $\kappa = 1.29$ typical for natural gas, we get $\beta = 3.10408$. To eliminate the fold in the equation, f_2 should be replaced with $H_{ad}\rho_{in}|P_{in} \to \max(P_{in}, P_{out}/\beta)$. It is convenient to divide the expression f_3 by $(2\pi\, rev)$ and consider the signature $\tilde{f_3} = M_{t,drv}(rev) - M_t$. As noted in [2], for drive equations to be stable it is necessary that $M_{t,drv}$ decrease with rev. Therefore, the first term in $\tilde{f_3}$ has the signature $(+0-)$, and the second already calculated $(+-0)$ in the region $P_{out}/P_{in} < \beta$, which gives the complete signature $(+--)$. Calculation of other derivatives is trivial. We also note that the presence of zeros in the signatures means that the

TABLE I
PATCH SIGNATURES OF PISTON COMPRESSOR [1]

patch	sgn	condition
f_1	$(+\ 0\ -)$	
f_2	$(+-0)$	$P_{out}/P_{in} < \beta$
f_3	$(+--)$	$P_{out}/P_{in} < \beta,\ \partial M_{t,drv}/\partial\, rev < 0$
f_4	$(+-0)$	
f_5	$(+-0)$	

TABLE II
PATCH SIGNATURES OF GENERIC COMPRESSOR [1]

patch	sgn	condition
f_1	$(+\ 0\ -)$	
f_2	$(+-0)$	$\partial z_{in}/\partial P_{in} < 0$ or small
f_3	$(+--)$	$\partial z_{in}/\partial P_{in} < 0$ or small

rule (1) is satisfied marginally, which is corrected by adding a regularizing ϵ-term to the element equation. Also, for the practical implementation of these formulas, it is necessary to introduce clamps, which force all variables to the working region: $Q_m \to \max(Q_m, 0)$, $P_{out}/P_{in} \to \max(P_{out}/P_{in}, 1)$, etc.

B. Generic compressors

Compressors of generic type can also be considered as an intermediate level of modeling (generic model). In this model, the variable rev is not introduced, and restrictions are imposed on other variables

$$f_1 = Q_{vol,max} - Q_{vol} \geq 0, \quad (15)$$
$$f_2 = H_{ad,max} - H_{ad} \geq 0, \quad (16)$$
$$f_3 = Perf_{max} - Perf \geq 0, \quad (17)$$

with constant $Q_{vol,max}$, $H_{ad,max}$ and $Perf_{max}$.

Stability analysis: calculating derivatives similarly, for $Q_{vol} = Q_m/\rho_{in}$ we have signature $(-0+)$, hence $(+0-)$ for f_1, see Table II. For $H_{ad} = RT_{in} z_{in}/(\mu_{in}\alpha)((P_{out}/P_{in})^{\alpha} - 1)$ we get $(*+0)$, where $* = \partial(z_{in}((P_{out}/P_{in})^{\alpha}-1))/\partial P_{in} < 0$. For an ideal gas $z = 1$, hence, obviously, $* = -$. For natural gas z is a decreasing function of P, in this case also $* = -$. For some gases, such as hydrogen, z may increase with P, but it remains close to 1 and changes so slowly that the remaining decreasing dependence of H_{ad} on P_{in} dominates. Under these conditions, f_2 has signature $(+-0)$. For $Perf = Q_m H_{ad}/\eta$ the signature $(-++)$ under the same conditions on z_{in}, thus f_3 has the signature $(+--)$.

C. Turbocompressors

Detailed modeling of turbocompressors was done in [2], [6], [7]. For the sake of completeness, here we review the main results.

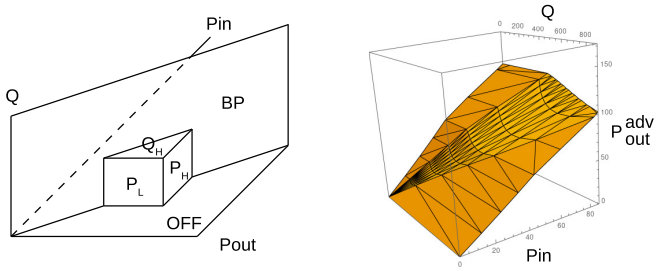

Fig. 2. Compressor modeling: 'free' model on the left; 'advanced' model for typical turbocompressor on the right. Images from [4], [7].

The equation of advanced patch has the form

$$f_1 = -P_{out} + P^{adv}_{out}(\hat{P}_{in}, \hat{Q}) \quad (18)$$
$$+ \min(P_{in} - P^{adv}_{in,min}, 0) + \max(P_{in} - P^{adv}_{in,max}, 0) \quad (19)$$
$$+ \min(-Q + Q^{adv}_{max}, 0) + \max(-Q + Q^{adv}_{min}, 0)), \quad (20)$$
$$\hat{P}_{in} = \min(\max(P_{in}, P^{adv}_{in,min}), P^{adv}_{in,max}), \quad (21)$$
$$\hat{Q} = \min(\max(Q, Q^{adv}_{min}), Q^{adv}_{max}). \quad (22)$$

The main part (18) is the equation $-P_{out} + P^{adv}_{out}(P_{in}, Q) = 0$, defined in rectangular region $P_{in} \in [P^{adv}_{in,min}, P^{adv}_{in,max}]$, $Q \in [Q^{adv}_{min}, Q^{adv}_{max}]$, with derivatives $\partial P^{adv}_{out}/dP_{in} > 0$, $\partial P^{adv}_{out}/dQ < 0$. Additional terms (19,20) carry out a continuous extension of this equation outside the region, with the same signs of derivatives. The resulting function $P^{adv}_{out}(P_{in}, Q)$ in typical case is shown in Figure 2 on the right. This surface represents the union of $rev \leq rev_{max}$ and $Perf \leq Perf_{max}$ patches converted into the space of transport variables. This conversion is done in the following way.

Step 1: calibration of the compressors and their drives with (bi-)quadratic functions:

$$H_{ad} = \sum_{ij} A_{ij} v^r_i v^q_j,\ \eta = \sum_{ij} B_{ij} v^r_i v^q_j, \quad (23)$$
$$Q_{vol,min} = \sum_i C_i v^r_i,\ Perf_{max} = \sum_i D_i v^r_i, \quad (24)$$
$$v^r = (1, rev, rev^2),\ v^q = (1, Q_{vol}, Q^2_{vol}), \quad (25)$$

with constant coefficient matrices A, B, C, D.

Step 2: definitions (4-6) are partially resolved until formulas in the (Q_m, ρ_{in}, H_{ad}) coordinate system are obtained, independent of temperature and gas composition:

$$Q_m = Perf_{max}\eta/H_{ad},\ \rho_{in} = Q_m/Q_{vol}, \quad (26)$$

Step 3: definitions (4-6) are finally resolved until formulas in the (Q_m, P_{in}, P_{out}) coordinate system are obtained, taking into account temperature and gas composition:

$$P_{in} = EOS_{inv}(\rho_{in}),\ z_{in} = P_{in}/(\gamma\rho_{in}), \quad (27)$$
$$P_{out} = P_{in}(H_{ad}\alpha/(\gamma z_{in}) + 1)^{1/\alpha}.$$

Here $\gamma = RT_{in}/\mu$ and the equation of state $\rho = EOS(P)$ is inverted to determine P_{in}.

Step 1 is performed once in the calibration procedure using fitting methods. Step 2 is also performed once, while the

domain of definition of functions on the (Q_{vol}, rev) plane is triangulated, the corresponding formulas are applied at the nodes, and linear interpolation in triangles is used for the continuous representation. Only step 3 is performed during simulations, as part of the procedure that determines the temperature and gas composition.

Stability analysis: consists in checking that the normals to the triangles used to represent the functions point to the octant corresponding to the correct signature. It suffices to carry out such a check in the coordinate system corresponding to step 2, while step 3 consists in a monotonic reparametrization of the axes that preserves the signature of the normal.

Further details: in order for the compressor to work properly, the flow through it must satisfy certain restrictions. On the $Q_{vol} = Q_{vol,min}$ line, the bypass regulator (rbp1,2 on Figure 4 bottom) is activated at the compressor, through which the flow can circulate, thereby ensuring the minimum required flow through the compressor (surge line). Since in this case the total flow through the compressor and the regulator may be less than this minimum value, this boundary is modeled by continuing the surface shown in Figure 2 on the right side along the Q axis towards small values. On the other side, there is a line $\eta = \eta_{min}$ (choke line), which is modeled by the continuation of the surface along the Q axis towards larger values. Since the compressor does not work efficiently on this part of the surface, the working point in this region is accompanied by a warning, and getting there should be avoided by adjusting the parameters. In addition, the continuation of the biquadratic functions into this region would lead to the formation of folds, and their replacement by the ruled continuation solves this problem. Switches similar to the surge line also occur on the $rev = rev_{min}$ line. At the same time, the location of the working point on this line and simultaneously on $Perf = Perf_{max}$ patch also leads to the formation of folds, which for typical compressors are outside the physical area and are eliminated by cutting.

The characteristics of the compressor drive can also depend on the ambient temperature T_{amb}, which can be modeled by constructing the biquadratic formula $Perf_{max}(rev, T_{amb})$. In this case, the resulting dependence in step 2 is linear in $Perf_{max}$, which leads to the possibility of precomputing the surface for three values of T_{amb} and then taking into account the dependence on T_{amb} using linear weighting with weights quadratically dependent on T_{amb}.

Compressor stations: are formed, in the simplest case, when individual compressor units are connected in parallel or in series. Examples of such combinations are shown in Figure 3a,b and in more detail in Figure 4 bottom. In this case, the type and controlled values of each compressor may be the same, they may also be different. The station also includes other elements, some of which (valves, shortcuts) have trivial functions. To ensure the stability of the solution algorithm (in particular, no cycles from shortcuts, indefinite pressure in the sequence of closed valves, etc.), such elements are eliminated in the preprocessing procedure. There are also other elements: coolers that affect temperature distributions inside and outside of stations and bypass-regulators providing a non-zero flow through the compressor. Parallel and serial connections of compressors can also create solution ambiguities, detailed below.

IV. Sensitivity and Principal Component Analysis

Below, Sensitivity Analysis and Principal Component Analysis of gas transport simulations will be considered.

A. Sensitivity Analysis

Determining the sensitivity of a model to changing parameters is a standard tool for in-depth analysis of simulation results. Usually it consists in the computation of sensitivity matrix $S^x_{ij} = \partial x_i/\partial p_j$, defined in terms of partial derivatives, along with the Jacobi matrix $J_{ij} = \partial y_i/\partial x_j$ and the sensitivity of the equations in terms of the parameters $S^y_{ij} = \partial y_i/\partial p_j$. Here x are model variables that also represent the simulation result, p are model parameters, y are equations in terms of which the model is formulated. With a small number of parameters, the derivatives can be found using the numerical differentiation algorithm:

init: simulate $p \to x$
for j=1,num(p) do
  variate parameter $\tilde{p}_j = p_j + dp_j$
  simulate $\tilde{p} \to \tilde{x}$
  differentiate $S^x_{ij} = (\tilde{x}_i - x_i)/dp_j$
done

or a similar algorithm with the choice of the central difference scheme. The differentiation step dp_j must be chosen reasonably, it must be small enough that the variation of dx_i can be considered linear, and large enough that this variation exceeds the numerical error of the simulation result. It is usually sufficient to perform several variations of different orders and verify that these properties are satisfied, using 1D plots $\tilde{x}_i(dp_j)$ for several key variables. The 'for' loop in this algorithm can be parallelized on several processors, providing a significant speedup for the analysis procedure. Alternatively, if there is an access to derivatives of equations with respect to variables and parameters, the sensitivity matrix can be found by solving the linear system

$$\sum_j (\partial y_i/\partial x_j)(\partial x_j/\partial p_k) + \partial y_i/\partial p_k = 0, \quad (28)$$

$$\sum_j J_{ij} S^x_{jk} + S^y_{ik} = 0, \quad (29)$$

which does not require additional simulations. However, often the simulation algorithm is encapsulated inside a software module where information about derivatives is not available. Also, sometimes the simulation algorithm is not a classical solution of a unified system of equations, but includes external iterations, relaxation procedures and/or calls to external 'black box' software modules. In this case, only the numerical differentiation algorithm described above remains for SA.

B. Principal Component Analysis

In the case of a large number of variables, equations and/or parameters, it makes sense to use PCA. In this approach, several components can be calculated, represented as linear combinations of variables that make the main contribution to the relations of the considered model. Technically, Singular Value Decomposition (SVD) of the respective matrices is performed for this purpose. Here we illustrate the application of PCA/SVD to the Jacobi matrix: $J = u\lambda v^T$, with a diagonal matrix λ and orthogonal matrices u and v. The largest eigenvalues λ correspond to the strongest dependencies. In this case, the corresponding left eigenvectors, columns of the u matrix, correspond to most rapidly changing combinations of y equations, and the right eigenvectors, columns of the v matrix, correspond to combinations of x variables with the strongest dependencies. To study the stability of numerical solution algorithms, it is also useful to know the smallest eigenvalues λ, which correspond to the weakest dependencies. In this case, the left eigenvectors represent linear combinations of equations that change little at a normalized change of all variables, and the right eigenvectors represent combinations of variables on which all equations weakly depend.

In the presence of small eigenvalues, algorithms for solving nonlinear systems, such as Newton's method, lose their convergence [11]. Mathematically, at a zero eigenvalue, the solutions of a linearized problem lose their uniqueness – the solutions either disappear or a continuous set of equivalent solutions appears. In practice, the solution of nonlinear systems is made with some given accuracy, which defines the ball of admissible solutions in the y-space, $|y| < tol_y$, using the l^2-norm. The preimage of this ball in x-space is the error ellipsoid, $dx = J^{-1}y$. The SVD of J-matrix determines the sizes of the semiaxes of the ellipsoid $|\delta x_i| = tol_y/\lambda_i$, while the right eigenvectors determine the orientation of the ellipsoid. For small eigenvalues, a strongly prolate ellipsoid arises corresponding to large x-errors, and in the $\lambda \to 0$ limit, to indifferent directions in the x-space.

Note that the error ellipsoid with large semiaxes is an indicator of instability in the solution of the problem. With variations in the problem statement, such as the choice of a starting point, parameters of iterative procedures, as well as with small variations in the free parameters of the modeling, the number of performed iterations may change. In this case, the end point makes jumps inside the y-ball, in practice can be considered random. As a result, the solution of the problem randomly changes within the x-ellipsoid. Large random variations of the solution indicate the ambiguity, which manifests both at the modeling level and in the physical system itself.

Application of PCA/SVD methods in gas transport problems was carried out in our recent work [3]. Here we will review the main results, now including the implementation details and modes of usage of these methods.

Implementation of PCA for large scale problems: large problems are usually represented by sparse matrices. The technical difficulty of SVD for large sparse matrices is that the result is generally a dense matrix, which makes computation time and memory requirements problematic. In special cases, when it is required to calculate not all, but only a few largest or smallest eigenvalues and the corresponding eigenvectors, there are algorithms that can keep the problem in a sparse class and represent the result in an economical form.

We use *Mathematica V12* for the described calculations, where the standard `SingularValueDecomposition` method is available. For full decomposition this method converts sparse matrices to dense by default. In a special case, if not all eigenvalues are required, but a small number of the highest ones, the method works in the sparse class. However, our analysis does not require the highest, but the lowest values, with which, according to the description, the method does not work.

This problem can be resolved as follows. Computing the product $J^T J$, we get a sparse symmetric positively semi-definite matrix. Its eigenvectors coincide with the columns of the v-matrix, and its eigenvalues coincide with the squares of the SVD eigenvalues. For this matrix, in *Mathematica V12* one can use the `Eigensystem` method, which works for the sparse case and allows one to restrict the computation to several lowest eigenvalues and corresponding eigenvectors. The same method, Arnoldi iterations, is used in *Arpack* system. To find u-vectors, one can find the product JJ^T and repeat the decomposition.

Note that for nonlinear systems, the linearization-based error estimate gives only an approximate result, more accurate for small δx and less accurate for large ones. For piecewise linear systems, this estimate is valid up to the cell boundary, where exact linearity is maintained.

Usage of PCA: according to the analysis, the result of simulation turns out to be not just a point in the space of variables, but a point with an error ellipsoid. This makes it possible to classify variables into more / less accurately defined and possibly completely inaccurately defined due to degenerations in the system. Other types of analysis should also take into account this information. For example, in the above considered SA, it may turn out that some variables undergo strong changes, jumps with a continuous change in parameters. This may not mean that these variables are highly sensitive to parameters, but that they change randomly within the error ellipsoid.

Another example of using PCA is the comparison of *simulation vs experiment*. The measurements have their own error ellipsoid, simulation and experiment results are compatible if these ellipsoids intersect. In practice, it is necessary to check the correspondence also at the 2-3-σ level and increase the ellipsoids by the appropriate factor.

Likewise, when comparing simulation results from *two different solvers*, one must check the intersection of their error ellipsoids. In the case if it is known in advance that the modeling used in the two solvers is the same, then it is enough to check that the $|y| < tol_y$ condition is satisfied for both of them, then both solutions will automatically belong to the common error ellipsoid. If it is not known whether

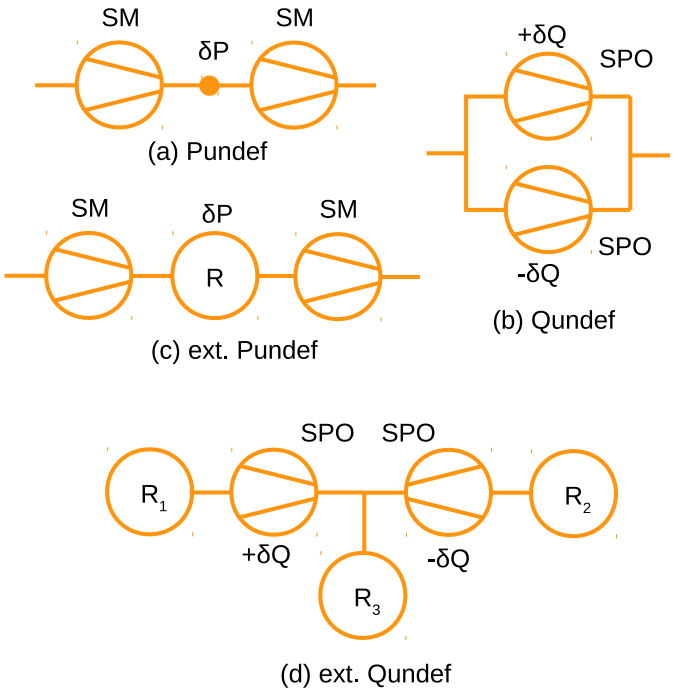

Fig. 3. Instabilities in gas transport problems: (a) undefined intermediate pressure in serial connection of SM-compressors; (b) undefined flow balance in parallel connection of SPO-compressors; (c,d) extended versions of the instabilities. Images from [3].

the modeling is the same, then cross-validation should first be carried out, substituting the answer of one solver into the evaluation function of another. If the $|y| < tol_y$ condition is violated, then it is possible to find out which y-components have large deviations, thus, which aspects of modeling differ between the solvers.

V. Solving nearly degenerate systems

As shown by the theoretical analysis and the numerical experiments below, stationary gas transport problems can possess instabilities. They are associated with the modeling of control elements, such as the compressors. While the advanced modeling is usually stable, the source of instabilities is the free model.

The simplest types of instabilities were discussed in [3] and shown here in Figure 3. In case (a), two serially connected SM compressors are considered. For such compressors, the control equation (3) is set to the value of specified mass flow, $Q_H = SM$. Since the flow through the compressors is the same, the equation $Q = SM$ is applied twice, which leads to the degeneration of the system. Because one equation is actually wasted, one continuous degree of freedom appears in the solution of the system. This degree of freedom corresponds to an undefined value of pressure between the compressors, which is not constrained by any equations. In case (b) there are two parallel SPO compressors. For such compressors, the equation for output pressure is doubled, $P_{out} = SPO$, the flow balance dQ through the compressors is undefined. In these two cases, the instability is localized within the compressor station. Instability can also go beyond the station. In case (c) there is a resistive subsystem between the two SM compressors, in which the pressure values appear to be undetermined. In case (d), two SPO compressors with a common output produce flow imbalance over wide areas of the network.

The situation is complicated by the following factors. The compressors do not have to be of the predefined type SPO/SPI/SM. They may formally belong to another type, but be on one of the faces of the surface for free model Figure 2, a face that actually corresponds to the conflicting type. Thus, the conflict may include faces corresponding to $P_H = POMAX$ and $P_L = PIMIN$; $Q_H = QMAX$ and $Q_L = QMIN = 0$, etc. The presence of the advanced part of the modeling does not solve the problem, since the advanced model (8) contains all the faces of the free model (3), which continue to generate conflicts on solutions. Other control elements that have similar modeling (regulators, flaptraps, etc.), as well as nodes with a fixed pressure or flow (Pset, Qset) can also participate in the conflicts. It is clear that it is impossible to foresee all conflicting combinations of faces in the control equations, due to combinatorial reasons. We have to look for special methods for solving degenerate systems that could be applied to this case. The potentially useful methods have been briefly listed in [3], now we consider them in full detail.

Regularization: is performed by the ϵ-term in free model equation (3). The reason for its introduction is that the equation at $\epsilon = 0$ satisfies the signature condition (1) only marginally, some derivatives vanish. The geometric interpretation of this is that the normals to the faces of the polyhedron shown on Figure 2 left are directed strictly along the axes, although they should be directed inside the octant described by the condition (1). Such marginality leads to degeneracy of the Jacobi matrix, ambiguity of solutions, bad condition numbers, and other troubles for the numerical solution procedure. The introduction of a regularizing ϵ term formally eliminates this problem by making the condition (1) strictly satisfied. At the same time, adjusting this parameter represents a compromise between the physical accuracy and the numerical stability of the solution procedure. In practice, the values $\epsilon = 10^{-6}...10^{-3}$ are tolerable, meaning the relative violation of, e.g., SPO-condition, up to 0.1%, simultaneously keeping the convergence rate near 100%.

Relaxed Armijo rule: it is clear that part of the problem is related to the line search algorithm [11]. According to this algorithm, in the process of system solving, a step is taken along the Newtonian direction $dx_N = -J^{-1}y$, not completely, but so that the residual of equations $|y|$ made a sufficient reduction. In [7], it was proposed to relax this requirement, allowing a controlled small increase of residual in nearly degenerate cases. Indeed, in practice this leads to a drastic improvement in the stability of the algorithm and a decrease in the number of iterations. The drawback is that, in rare cases, Newtonian iterations go in cycle. Theoretically, the conditions for the convergence of Newtonian iterations [11] require the exact fulfillment of the Armijo rule. Thus, the rule relaxation

is an empirical method that often improves convergence in degenerate problems, but does not work in 100% of cases.

Topological reduction: the method described in [7] makes it possible to contract parallel and serial stations, eliminating the degenerate degrees of freedom contained in them, which leads to an increase in the stability of the solution algorithm. However, this method only works for local conflicts and cannot resolve the extended ones.

Dynamical problems: algorithms for integrating dynamical systems used to obtain stationary states can be more stable than the straightforward solution of stationary problems. Indeed, *Pundef*-conflicts can be resolved, since the intermediate pressure values are determined by the starting point and the integration process. These values are still arbitrary, but this arbitrariness does not complicate the process of finding a solution. *Qundef*-conflicts can be resolved similarly by including the corresponding kinetic terms in the equations.

Homotopic methods: this class of methods [20] considers the deformation of equations from some simple solvable form to the required form, in which the trajectory of the solution is continuously tracked. For example, the linear deformation $y = y_0(1-\alpha) + y_1\alpha$ can be used, with $\alpha \in [0,1]$. The problem with such methods is the possible appearance of a fold in the equations, leading to a loss of the solution. In our particular case, when using regularization, the required equations are guaranteed to have a unique solution. As an auxiliary form, one can use a linear non-degenerate system, which also has a unique solution. However, this does not mean that the mixed system will also have a unique solution. It is easy to construct examples of matrices that have a determinant of one sign, for which a linear combination with positive coefficients has a determinant of another sign, or equal to zero. In this case, it makes sense to use the structure of the system, for example, do not touch the Kirchhoff equations and deform only the equations of the elements. It is clear that only singular equations need to be deformed, since the rest keep the Jacobi matrix nondegenerate and present no problems. Then this method becomes equivalent to our ϵ-regularization with a gradual decrease in the ϵ parameter. Theoretically, this method in its last stage is unstable, since an increasingly degenerate system is being solved. Our numerical experiments presented below show that the described homotopy method works as a stabilizer, although not in 100% of cases.

Note also that the linear deformation of equations described above is only the simplest version of the homotopic method. The work [20] offers tools to overcome $rank\ J = n-1$ degeneracy by extending J from $n \times n$ to $n \times (n+1)$ full-rank matrix. However, our system typically have multiple zero eigenvalues. The described methods do not seem to work immediately for this case, at higher order degeneracy requiring an increasingly complex parameterization.

Piecewise linear systems: for such systems, the space of variables is divided into polyhedral cells, in each the system is linear, with continuous connection at the boundaries. For such systems, there are methods that allow finding a solution in a finite number of steps, see [8]–[10] and also [20] Chap. 12-15. It is noteworthy that some of these methods work even if the system is piecewise degenerate. In algorithm [9], it is proposed to follow the Newtonian direction in non-degenerate cells, or opposite one, dependently on the sign of Jacobian. In degenerate cells, it is proposed to follow the right annulator of the system matrix. Each time, the movement should stop at the border of the next cell. Such algorithm has theoretically guaranteed convergence [9]. For our applications, this algorithm should be extended to nonlinear systems. The annulators can be found using fast procedures (*Mathematica, Arpack*).

Pseudo-inverse: a related SVD-based algorithm is the procedure for finding the Newtonian step $dx_N = -J^{-1}y$ with elimination of zero eigenvalues, see Chap. 2.6 in [21]. In practice, to find the pseudo-inverse J^{-1}, after SVD, all non-zero eigenvalues are replaced by inverse $\lambda \to \lambda^{-1}$, and zero ones remain unchanged: $0 \to 0$. If the problem would be globally degenerate, this procedure would provide sliding along a trajectory orthogonal to the annulators, ignoring degenerate combinations of equations and unstable variables, concentrating only on changing the essential variables in the system. It is not known whether there is a generalization of this algorithm to the nonlinear piecewise degenerate case, that is of interest for our applications.

Among the described methods, the empirical approach with ϵ-regularization, relaxed Armijo rule and optional error calculation by PCA method works satisfactorily in practice. Among the most promising approaches, we consider the extension of the described methods to dynamic problems.

VI. Numerical experiments

A number of numerical experiments have been performed to test the performance of above described methods.

A. Test networks

We use the stabilized Newton algorithm described in [4] to solve the gas transport problems on the following networks. A small network N1 has been created by us to test functionality of various elements, shown in Figure 4 on the top. A medium size network ME, created in frames of the project *MathEnergy*, containing all features of realistic networks, shown in Figure 4 on the center. A set of large scale realistic networks N85, given to us by our industrial partner for benchmarking of the methods. The main parameters of all test networks are contained in the Table III.

B. Test of piston and generic compressors

Since their implementation is a main contribution of the paper, we have tested the stability and performance of the solver for the networks containing such elements. In particular, the network N1 has 100 nodes and 111 edges, of which 4 compressors are organized into two compressor stations c1|2 and c3|4 with individual compressors connected in parallel, as shown in Figure 4 at the bottom. Compressors in station c1|2 are configured as piston ones, in station c3|4 as generic ones.

TABLE III
PARAMETERS OF TEST NETWORKS [2]

network	tot.num.	nodes	edges	pipes	compressors	regulators	Psets	Qsets
N1	1	100	111	34	4	4	2	3
ME	1	437	482	370	20	24	3	164
N85/L	23	3232-3886	3305-3974	2406-2835	1-7	59-77	6-7	625-843
N85/H	62	2914-3818	2989-3952	1498-1937	16-42	59-107	5-9	328-505

Values P_H, Q_H are set to unreachable high values, thereby activating the f_i patches described above.

The procedure consists of several phases with a gradual increase in the modeling level. At first, the compressors are set to fulfill the main target values, e.g., $P = P_H$, then the modeling level (3) is used, taking into account additional conditions, then the modeling level (8) is taken. The solution procedure described in [5] consists of the translation phase of the system from the network description language to the language understood by the numerical solver, and the actual numerical solution phase. In this test, approximately the same results are obtained if turbocompressors are used instead of piston/generic ones. These numerical experiments show that the inclusion of piston and generic compressors in the system does not lead to any divergences or slowdown of the solution procedure, which is a direct consequence of the implementation of the stability criteria described above.

We also performed numerical experiments with test networks from N85 set. This set contains 85 networks with complexity up to four thousand nodes and up to 42 compressors. Among them are multiple piston and generic compressors, in parallel and series connections. We have found that the presence and placement of such compressors does not affect performance in any way, and this is consistent with the convergence conditions we developed.

C. Test of ϵ-homotopy

The dependence of the convergence of network problems on the ϵ-parameter was investigated in [3] on N85 networks for free compressor setting. In the present work, we have carried out such a study for advanced compressors. In addition, we have included an external iterative loop in the solution algorithm, the so-called mix-iteration, in which the gas composition, temperature, parameters of the refined equation of state, etc. are calculated. Here we have taken the opportunity to explore a simple homotopy algorithm by inserting parameter division into the mix-iteration: $\epsilon \to \epsilon/q$, $q > 1$. The simulation results are shown in Tables IV and V. In accordance with the above considerations, as the ϵ-parameter decreases, the problem becomes more and more degenerate. In total across all N85 networks, the number of divergent scenarios and the computation time increase with decreasing ϵ-parameter. For the homotopy algorithm, we performed two numerical experiments. Both started at $\epsilon = 10^{-3}$ and ran 10 mix-iterations. In one experiment, $q = 2$ was chosen and the homotopy was carried out up to the value $\epsilon \sim 10^{-6}$. The algorithm is slightly more stable, leaving divergent 2 scenarios out of 85, compared to simply fixing ϵ to a final value, which makes divergent 3 scenarios. In the second experiment, $q = 4$ was chosen and the division was carried out up to the deeper value $\epsilon \sim 10^{-9}$. Here, the homotopy algorithm turns out to be much more stable, although it still leaves divergent 10 scenarios out of 85. Since the value of $\epsilon = 10^{-6}$ is sufficient for practical purposes, we conclude that the described homotopy algorithm stabilizes the solution of the problem, with moderate success.

D. Sensitivity Analysis of N1 network

It is carried out by us in order to test the algorithm described above and the software module based on it. For this test, in each of the two compressor stations c1|2 and c3|4, one compressor was configured as specified output pressure (SPO), the other as specified mass flow (SM). The results are shown in Figure 5. In case (a), input pressure in n99 supply is changed for 1 bar. The resulting variation of pressure does not propagate beyond the nearest compressor station c3|4. In case (b), SPO in c1 compressor is changed for 1 bar. The change propagates further to the network. The maximum dP is reached in the consumer n76. The increase of dP is due to nonlinearity of pipe friction law. In case (c), SM in c4 compressor is changed for 2%. The result corresponds to a different balance of flows in the network, while the pressure is changed insignificantly.

Thus, the application of SA to the N1 network shows that of the three parameter variations considered, the resulting pressure in the network is sensitive to only one parameter, SPO in c1 compressor.

E. Principal Component Analysis of ME network

It is carried out to test the performance of the method on a larger network than in our earlier study [3]. This early study looked at N1 network with compressors in free SPO mode. There, PCA revealed two small eigenvalues that varied proportionally to the ϵ parameter and corresponded to conflicts within the stations. A larger small eigenvalue was also found, corresponding to an extended conflict between compressor stations. In the current work, for the ME network, we obtain

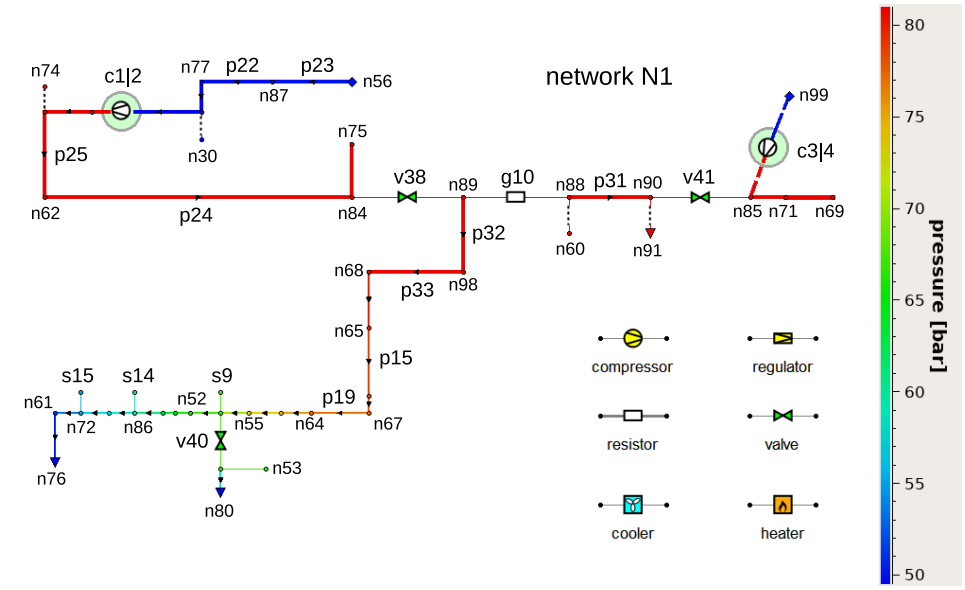

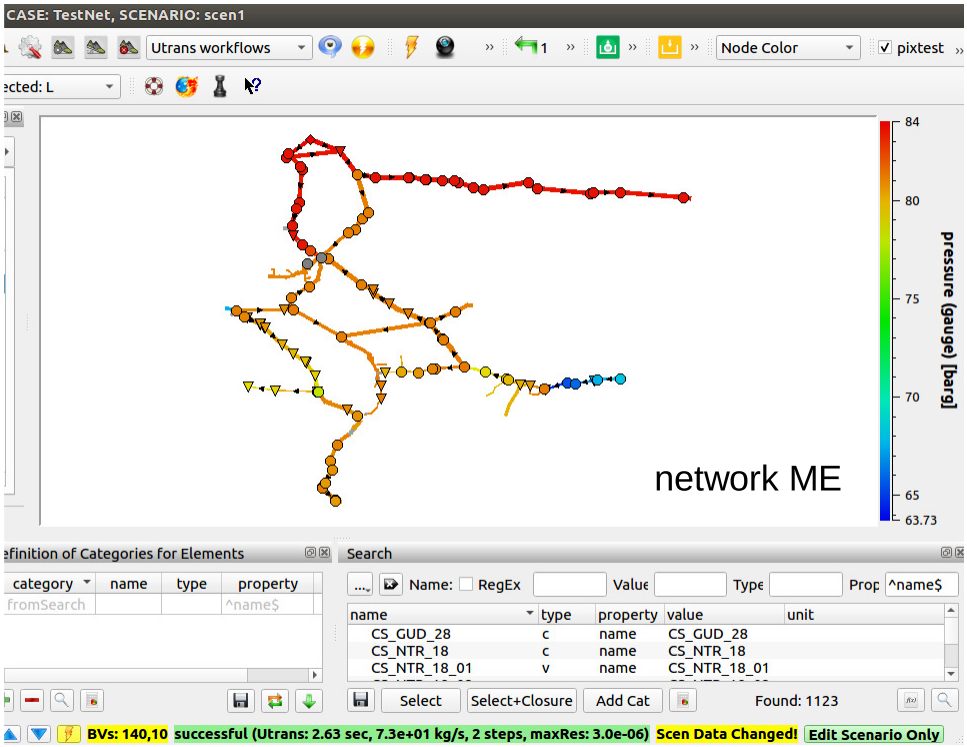

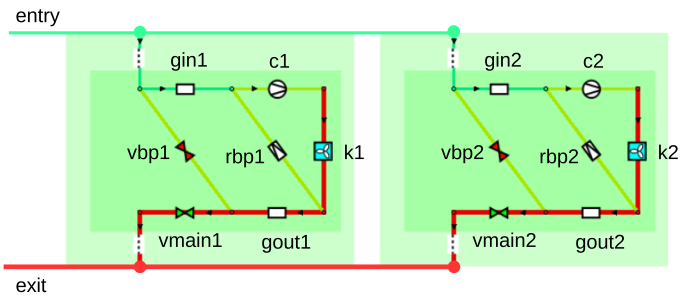

Fig. 4. On the top: test network N1; in the center: test network ME; at the bottom: the structure of parallel compressor station. Images from [2], [4].

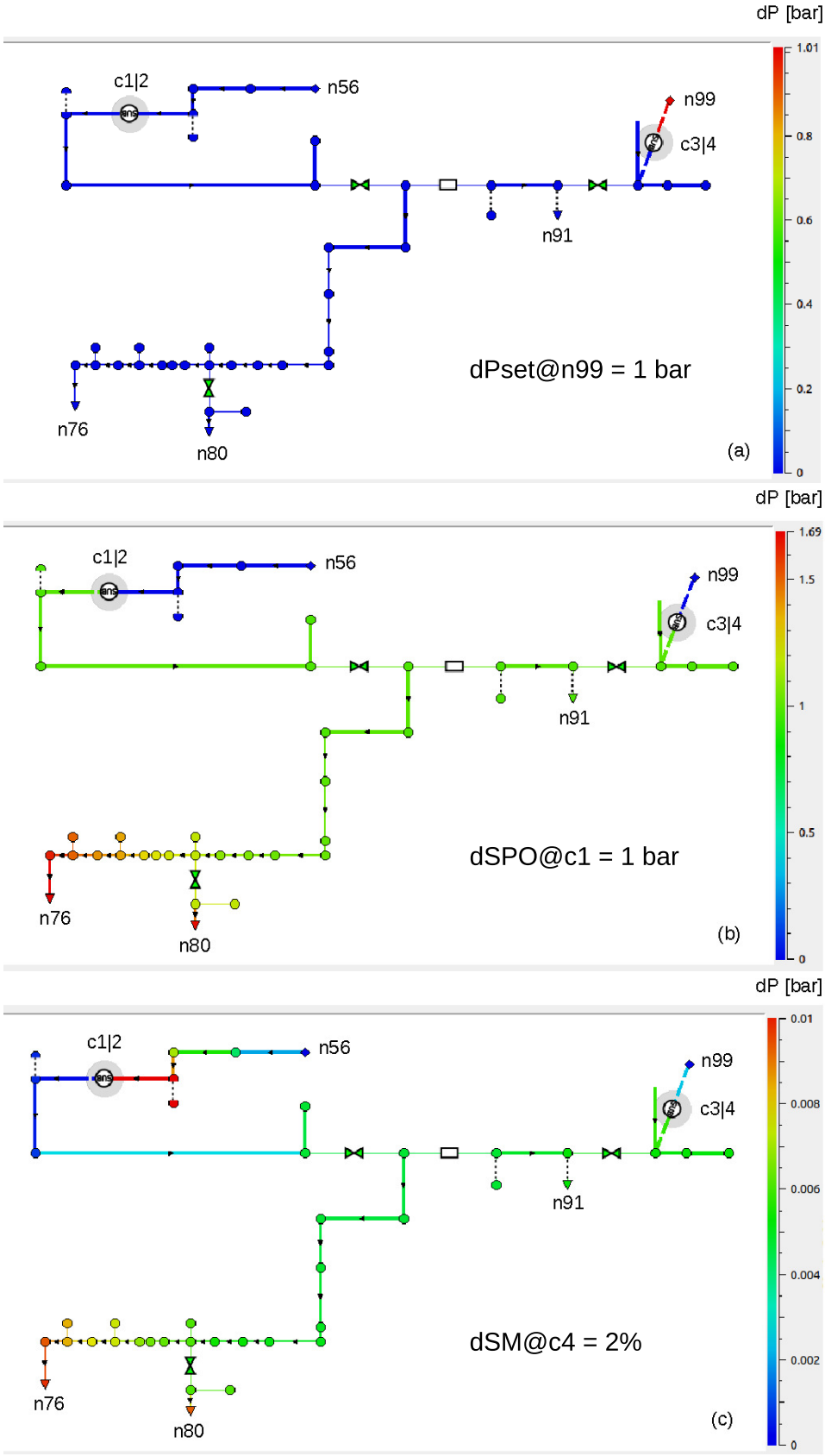

Fig. 5. Sensitivity Analysis, for N1 network.

TABLE IV
CONVERGENCE FOR FIXED ϵ, N85 NETWORKS

ϵ	total div.	total time*
10^{-3}	1	84
10^{-6}	3	117
10^{-9}	40	533

* in minutes, for Intel i7 / CPU 2.6 GHz / RAM 16 GB computer.

TABLE V
CONVERGENCE FOR ϵ-HOMOTOPY, N85 NETWORKS

q	total div.	total time*
2	2	87
4	10	98
$\epsilon = 10^{-3}/q^n,\ n = 0...10$		

* in minutes, for Intel i7 / CPU 2.6 GHz / RAM 16 GB computer.

the results presented in Tables VI-VIII. Initially, the value of the parameter $\epsilon = 10^{-3}$ was selected, all compressors were set to free SPO mode.

The results obtained indicate another type of conflict, that is related to pipes. The lowest eigenvalue corresponds to a cycle of two pipes with lengths and diameters $L_{p0618} = 118m$, $D_{p0618} = 0.6m$, $L_{p0643} = 120m$, $D_{p0643} = 0.9m$, possessing a zero flow. The next largest eigenvalue corresponds to a cycle of three pipes with lengths $L_{p0110} = 136m$, $L_{p0765} = 1917m$, $L_{p0766} = 1967m$, common diameter $D = 0.8m$ and a small flow $m \sim 0.1$ kg/s. The left eigenvectors correspond to an indefinite flow circulating in cycles. The right eigenvectors for a given associated with pipes conflict are the same as the left ones. They correspond to the sum of equations taken over the cycle, which in leading order have the form [4]: $P_1|P_1| - P_2|P_2| = R_q Q|Q|$. When such a sum is taken, the P-terms disappear, leaving only the sum of the Q-terms (Kirchhoff's second law). The reason for the degeneracy is the low resistance R_q for short and thick pipes. Also, due to the quadratic dependence on Q, additional suppression occurs for small flows. Note that the complete expression for the friction equation in pipe also contains a laminar term. This term is linear in Q, but its value is insufficient to stabilize the system at low flows. Possible ways to solve this problem can be: artificial increase of the laminar term, similar to ϵ-regularization; replacing short pipes with shortcuts followed by contraction [6]; topological reduction of serial and parallel connections of pipes [7].

At higher eigenvalues, there are similar pipe-conflicts, while the conflicts associated with compressors and regulators also begin to occur. As the regularizing parameter decreases to $\epsilon = 10^{-6}$, one of these conflicts descends from the high eigenvalues $\lambda = 4.29 \cdot 10^{-4} \rightarrow 4.29 \cdot 10^{-7}$, proportionally following the change in ϵ by three orders of magnitude. At the same time, the eigenvalues and vectors of pipe-conflicts change little. This new conflict corresponds to the compressor and regulator connected by a series of 4 pipes with a total length of 35 km. On the solution, the compressor and regulator are closed, have zero flow. In this case, the pressure in the intermediate segment is undefined. Thus, the described conflict belongs to the extended type (c), shown on Figure 3.

In the simulations under consideration, the accuracy parameter $tol_y = 10^{-5}$ is used. The found eigenvalues correspond to the error in the x-space according to the formula $|\delta x_i| = tol_y/\lambda_i$. In our simulations, the range of operating values of pressures and flows is in the order of $P = 0{-}100$ bar, $Q_m = 0 - 100$ kg/s. Now it is clear that the first eigenvalue gives an error exceeding this range, and the corresponding degree of freedom is completely undefined. For the next eigenvalue, the error is about 4% and further decreases to $< 1\%$. Note also that for higher eigenvalues, the eigenvectors are distributed over a large number of elements, and the error in each element is even smaller.

Thus, an application of PCA to the ME network appears to be useful, bringing additional knowledge about the new type of conflicts, confirming the conclusions about the ϵ-regulated instabilities, and making a differentiated estimation of the simulation error for different degrees of freedom present in the solution.

TABLE VI
THE LOWEST EIGENVALUE AND RELATED PRINCIPAL COMPONENTS, FOR ME NETWORK

λ_1	$\lvert\delta x_1\rvert$	$\delta Q_{m,p0618}$	$\delta Q_{m,p0643}$	eq_{p0618}	eq_{p0643}
$2.56 \cdot 10^{-8}$	390	-0.707	-0.707	-0.707	-0.707

TABLE VII
THE SECOND LOWEST EIGENVALUE AND RELATED PRINCIPAL COMPONENTS, FOR ME NETWORK

λ_2	$\lvert\delta x_2\rvert$	$\delta Q_{m,p0110}$	$\delta Q_{m,p0765}$	$\delta Q_{m,p0766}$	eq_{p0110}	eq_{p0765}	eq_{p0766}
$2.46 \cdot 10^{-6}$	4.06	0.589	0.571	0.571	0.589	0.571	0.571

TABLE VIII
THE NEXT LOWEST EIGENVALUES, FOR ME NETWORK

λ_3	$\lvert\delta x_3\rvert$	λ_4	$\lvert\delta x_4\rvert$	λ_5	$\lvert\delta x_5\rvert$	λ_6	$\lvert\delta x_6\rvert$
$1.38 \cdot 10^{-5}$	0.725	$2.10 \cdot 10^{-5}$	0.477	$2.59 \cdot 10^{-5}$	0.386	$2.63 \cdot 10^{-5}$	0.380

VII. CONCLUSION

In this work, modeling of piston and generic type gas compressors was carried out. The signatures of the derivatives of the control equation are analyzed, the ranges of parameter values are identified, under which the conditions for the stable operation of the algorithm for solving stationary network problems are satisfied. After the practical implementation of the modeling, in numerical experiments on realistic gas networks, the convergence of the solution algorithm is shown.

In addition, an extended review was made of results on turbine type compressors, methods of Sensitivity and Principal Component Analysis applied to gas transport networks, methods for solving nearly degenerate nonlinear systems. A number of new numerical experiments were carried out on realistic scenarios of a stationary type, representing the application of these methods. In particular, it is shown that regularization methods, relaxed line search and ϵ-homotopy have a stabilizing effect on the solution procedure. Sensitivity and Principal Component Analysis show areas of increased system responsiveness to parameter variations and solution procedure setups. In addition to the already known conflicts associated with the compressor stations, there are flow ambiguities in cycles of short pipes. All the effects observed in numerical experiments are in agreement with the theoretical analysis.

Our future plans include extending the described methods to dynamic problems.

ACKNOWLEDGMENT

The work has been supported by the project TransHyDE-Sys, grant 03HY201M.

REFERENCES

[1] A. Baldin et al., “Solving Stationary Gas Transport Problems with Compressors of Piston and Generic Type”, in Proc. of INFOCOMP 2022, International Conference on Advanced Communications and Computation, pp. 1-5, IARIA, 2022.

[2] A. Baldin et al., “AdvWarp: a transformation algorithm for advanced modeling of gas compressors and drives”, in Proc. of SIMULTECH 2021, International Conference on Simulation and Modeling Methodologies, Technologies and Applications, pp. 231-238, SciTePress, 2021.

[3] A. Baldin et al., “Principal component analysis in gas transport simulation”, in Proc. of SIMULTECH 2022, International Conference on Simulation and Modeling Methodologies, Technologies and Applications, pp. 178-185, SciTePress, 2022.

[4] T. Clees, I. Nikitin, and L. Nikitina, “Making network solvers globally convergent”, Advances in Intelligent Systems and Computing, vol. 676, 2018, pp. 140-153.

[5] T. Clees et al., “MYNTS: Multi-phYsics NeTwork Simulator”, in Proc. of SIMULTECH 2016, International Conference on Simulation and Modeling Methodologies, Technologies and Applications, pp. 179-186, SciTePress, 2016.

[6] T. Clees, I. Nikitin, L. Nikitina, and L. Segiet, “Modeling of gas compressors and hierarchical reduction for globally convergent stationary network solvers”, International Journal On Advances in Systems and Measurements, vol. 11, 2018, pp. 61-71.

[7] A. Baldin, T. Clees, B. Klaassen, I. Nikitin, and L. Nikitina, “Topological reduction of stationary network problems: example of gas transport”, International Journal On Advances in Systems and Measurements, vol. 13, 2020, pp. 83-93.

[8] J. Katzenelson, “An algorithm for solving nonlinear resistor networks”, Bell System Technical Journal, vol. 44, 1965, pp. 1605-1620.

[9] M. J. Chien and E. S. Kuh, “Solving piecewise-linear equations for resistive networks”, International Journal of Circuit Theory and Applications, vol. 4, 1976, pp. 1-24.

[10] A. Griewank, J.-U. Bernt, M. Radons, and T. Streubel, “Solving piecewise linear systems in abs-normal form”, Linear Algebra and its Applications, vol. 471, 2015, pp. 500-530.

[11] C. T. Kelley, Iterative Methods for Linear and Nonlinear Equations, SIAM, Philadelphia, 1995.

[12] J. Mischner, H. G. Fasold, and K. Kadner, System-Planning Basics of Gas Supply, Oldenbourg Industrieverlag GmbH, 2011 (in German).

[13] M. Schmidt, M. C. Steinbach, and B. M. Willert, “High detail stationary optimization models for gas networks”, Optimization and Engineering, vol. 16, 2015, pp. 131-164.
[14] J. Nikuradse, “Laws of flow in rough pipes”, NACA Technical Memorandum 1292, Washington, 1950.
[15] C. F. Colebrook and C. M. White, “Experiments with fluid friction in roughened pipes”, in Proc. of the Royal Society of London, Series A, Mathematical and Physical Sciences, vol. 161, num. 906, 1937, pp. 367-381.
[16] P. Hofer, “Error evaluation in calculation of pipelines”, GWF-Gas/Erdgas, vol. 114, num. 3, 1973, pp. 113-119 (in German).
[17] J. Saleh, Fluid Flow Handbook, McGraw-Hill 2002.
[18] DIN EN ISO 12213-2: Natural Gas - Calculation of Compression Factor, European Committee for Standardization, 2010.
[19] O. Kunz and W. Wagner, “The GERG-2008 wide-range equation of state for natural gases and other mixtures: an expansion of GERG-2004”, J. Chem. Eng. Data, vol. 57, 2012, pp. 3032-3091.
[20] E. L. Allgower and K. Georg, Introduction to Numerical Continuation Methods, SIAM, Philadelphia, 2003.
[21] W. H. Press, B. P. Flannery, S. A. Teukolsky, and W. T. Vetterling, Numerical Recipes in C, Cambridge University Press 1992.